

# Relation between local density and density relaxation near glass transition in a glass forming binary mixture

D. C. Thakur,<sup>1</sup> Sandeep Kushawah,<sup>1</sup> Jalim Singh,<sup>1</sup> Anna Varughese,<sup>1</sup> and Prasanth P. Jose<sup>1, \*</sup>

<sup>1</sup>*School of Physical Sciences, Indian Institute of Technology Mandi, Kamand, Himachal Pradesh 175005, India*

Many investigations shed light on various correlations between structure and dynamics in supercooled liquids; however, a general relation between structure and dynamics remains elusive. This molecular dynamics simulation study identifies the interrelationship between the growth of the highest peak of the radial distribution function  $g(r)$ , variation in the radial force from this peak, and the slowdown of the density relaxation in the supercooled states of a model binary glass former. From the microscopic string-like motion in supercooled liquids, we argue that the surface density on a spherical shell  $\rho_{loc}$  around a reference particle at the highest peak of  $g(r)$  can represent the free volume available for motion. We further show from these arguments and simulations that density relaxation time  $\tau_\alpha$  and  $\rho_{loc}$  are connected,  $\tau_\alpha \propto \exp(\rho_{loc}/(\rho_0 - \rho_{loc}))$ , where dynamics diverge at  $\rho_0$ . This relation is similar to the Vogel–Fulcher–Tammann (VFT) relation in the supercooled liquids, thus giving insight into the structural origin of the VFT as jamming of particles in a channel of density relaxation.

Liquids undergo glass transition or acquire solid-like rigidity with marginal structural changes when compressed or cooled at a faster rate than structural relaxation. These solid-like domains are due to the transient cages that resist density relaxation. Recent experiments on two-dimensional (2D) colloids show molecular-cages have higher local density [1], whose size fluctuation facilitates the density relaxation [2]. Therefore, a microscopic theory of dense liquids can shed light on the relationship between the structure of molecular cages and slowing down the density relaxation. A perturbation theory of dense Lennard-Jones (LJ) liquids by Weeks, Chandler, and Andersen (WCA) propose that repulsive interactions govern the structure of dense liquids [3], which also suggest that the dynamics also follows the same [4]. A test of WCA theory in simulations of glass forming binary mixture on a model (well-known for the study of glass transition by Kob and Andersen (KA) [5, 6]) with (KA) and without attractive (KAWCA) interactions near the glass transition [7, 8] show that the density relaxation dynamics is remarkably slower, in the supercooled state with attractive interactions at the number density  $\rho = 1.2$ , while the density relaxation in KA and KAWCA models are nearly identical at the higher density  $\rho = 1.8$ . Studies also show that the relaxation dynamics become identical when the range of interaction includes the whole first coordination shell [9]; besides, the attractive and repulsive type of interactions together form the fluctuating potential of the molecular cage, irrespective of the type; identical cage potential leads to the same density relaxation [10]. Therefore, characterization of type, range, and depth of interactions of molecular cages in the viscous liquids give insight into the relationship between dynamics and local structure.

A comparison of forces in KA and KAWCA models shows that the difference between mean forces on particles are different when dynamics differ [11, 12]. Also, the configurational entropy obtained from the radial distribution

function  $g(r)$  [13] can identify differences in the dynamics, thus suggesting that  $g(r)$  governs relaxation dynamics [14, 15]. Moreover, insight from machine learning studies also supports the role of  $g(r)$  [16]. Interestingly, a recent study arrived at an exponential relation between the relaxation dynamics of the system and order parameter derived from the relative angle between atoms in the first coordination shell that is similar to Vogel–Fulcher–Tammann relation [17]. Therefore studies suggest that  $g(r)$  at the first coordination shell has a decisive role in the relaxation dynamics of supercooled LJ liquids. Moreover, the schematic mode-coupling theory uses the value of the structure factor at the first peak corresponding to the length scale of the nearest neighbor separation [18, 19], to calculate density relaxation time.

Many studies support the relationship between local structure and relaxation dynamics. Notably, there is a relation between the short-time  $\beta$  relaxation (inside the cages) and  $\alpha$  relaxation with both having identical temperature dependence [20], the information theory also confirms the role of local parameters in defining global dynamics [21]. Another study on gas-supercooled coexistence in polymers shows a correlation between density relaxation and particle distribution in the first coordination shell [22]. Many recent studies also show that local potential affect dynamics [23] in 2D systems that is explained from dynamic facilitation [24]; thus, suggest a relation between local structure and dynamics. The transient cage formation leads to an increase in local density [1] that reduces the available free volume for the molecules to relax. Thus suggest that the free-volume theory [25] can address the relationship between structure and dynamics. In the free-volume theory of a hard-sphere system, the density relaxation  $\tau_\alpha \propto \exp(Bv_0^*/v_f^*)$ , where  $v_f^* = v^* - v_0^*$  is the difference between mean free-space and self-volume [26]. A rough estimate of free volume in soft-potentials is Voronoi volume [27], many studies look into the detailed classification of the various forms

of free-volume, such as vibrationally accessible, hardcore free volume [28] *etc.*. This study deduces a relationship connecting the surface density  $\rho_{loc}$  of a spherical shell with radius  $r^*$  at the highest peak of  $g(r) \propto 1/v_f$ , where  $v_f$  is free-volume in the channels of density relaxation and the density relaxation time  $\tau_\alpha$ , from a systematic analysis of variation of  $\tau_\alpha$  and  $g(r^*)$  with temperature from the analysis of the trajectories from simulations.

*Methods:* Molecular dynamics simulations in this investigation use velocity Verlet algorithm [29] to integrate the equation of motion of  $N = 8000$  particles in a micro-canonical ensemble. The system simulated is the 4 : 1 binary mixture  $A$  and  $B$  defined in KA [5] and KAWCA [8] models. The KA potential as function of inter-particle separation  $r$  reads:  $V_{\alpha\beta}(r) = 4\epsilon_{\alpha\beta} \left[ (\sigma_{\alpha\beta}/r)^{12} - (\sigma_{\alpha\beta}/r)^6 \right] + K_{\alpha\beta}$ , where parameters are  $\alpha, \beta \in \{A, B\}, \epsilon_{AA} = 1.0, \sigma_{AA} = 1.0, \epsilon_{AB} = 1.5, \sigma_{AB} = 0.8, \epsilon_{BB} = 0.5,$  and  $\sigma_{BB} = 0.88$ [5]; arbitrary constant  $K_{\alpha\beta}$  ensures continuous potential at the cut-off. The potential cut-offs are  $2.5\sigma_{\alpha\beta}$  and  $2^{1/6}\sigma_{\alpha\beta}$  respectively for KA and KWCA models. The density range of the simulation is from  $\rho = 1.2$  to 1.8 in a grid of  $\delta\rho = 0.2$ ; in each density, temperatures form an uneven grid from high to low temperatures. The data presented in this study use Length, temperature, and time in units of  $\sigma_{AA}, \sigma_{AA}\sqrt{m/\epsilon_{AA}},$  and  $\epsilon_{AA}/k_B$ . The initial configuration is prepared at high temperatures for all densities and quenched to the desired temperature. The duration of equilibration is  $20 \tau_\alpha$  or higher at all temperatures.

We look at the first coordination shell in Figs. 1(a) and (b) around a reference particle to arrive at a relation between  $g(r)$  and the available free volume, where there is crowding of nearest neighbors in potential energy minima. The string-like motion in the supercooled liquids [30–33] is a prominent microscopic mechanism of rearrangement of particles in the typical arrangement of particles in the schematic diagram given in Fig. 1(b), where atoms move among nearly identical environments with a slight expansion of the shell [2]. The string lengths enhance as temperature reduces in a supercooled liquid, [34]. The growth of the string lengths and the  $\tau_\alpha$  with reduction of temperature show similarity in simulation studies on the glass-forming supercooled polymers [35]. Many studies identify that the strings that are part of string-like motion are cooperatively rearranging regions [36–38] in theories of the glass-transition [19]. Earlier studies show a preference for string-like motion at low  $T$  is due to the high energy cost for the creation of a hole [39–41]. The dominant type of particle motion that contribute to the relaxation are pair moves marked by the black arrows in Fig. 1(b); many connecting pairs lead to the typical string-like or ring-like collective motion (green arrows in Fig. 1(b)) on a two-dimensional (2D) surface marked by the  $r^*$  which is common in the density relaxation of glasses [42]. The mean-field the-

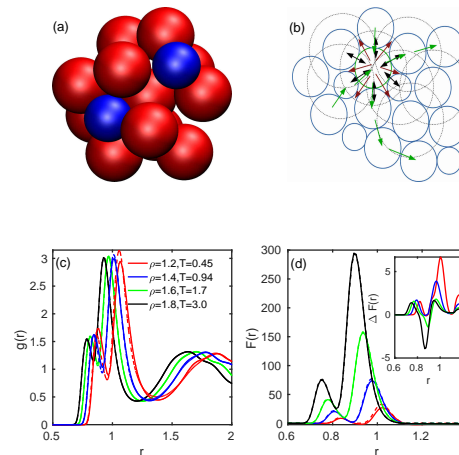


Figure 1. (a) Typical 3d of distribution of KA/KAWCA particles of a cage at  $\rho = 1.2$  ( $r_A \propto \sigma_{AA}$  and  $r_B \propto (\sigma_{AB} + \sigma_{BB})/2$ ). (b) The 2D schematic representation of (a) with A (big) and B (small). In (b): the green circle is the reference particle; the black double arrow is the preferred relaxation path; the red arrow is unfavoured relaxation path; the green arrows are the string-like collective motion; dotted circles mark the typical peak of  $g(r)$ . (c) radial distribution functions  $g(r)$ ; (d) corresponding variation in the average radial force  $F(r)$  in supercooled at typical supercooled states; (d)(inset) shows difference between  $F(r)$  of KAWCA and KA models  $\Delta F(r)$  at these state points.

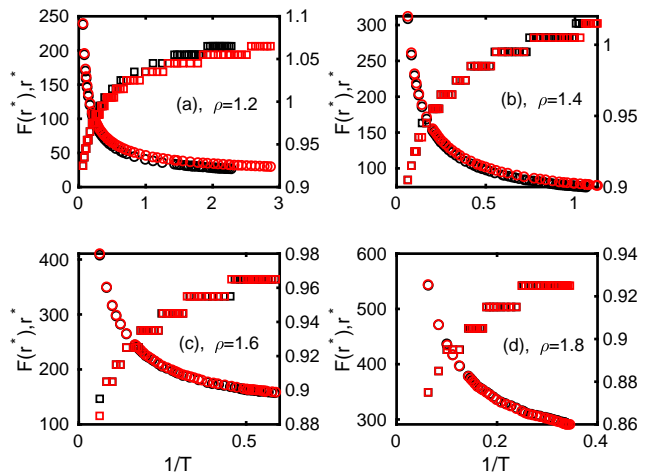


Figure 2. Left axis and  $\circ$  show variation of  $F(r^*)$  vs  $1/T$ . Right axis and  $\square$  shows variation of  $r^*$  (position of highest peak in  $g(r)$ ) vs  $1/T$ . The color black and red are for KA and KAWCA, respectively.

ory for polymers [39, 40, 43] show that the free-energy barrier for string-like motion  $E \propto v_m^{-1}$ , where  $v_m$  is the available free-volume. The quasi-linear paths of strings are along the inter-penetrating 2D surfaces marked as dotted circles in the one-dimensional (1D) projection in Fig. 1(b). The number density of particles along this path is proportional to a peak height of the  $g(r)$ , which increases with the reduction of the temperature due to

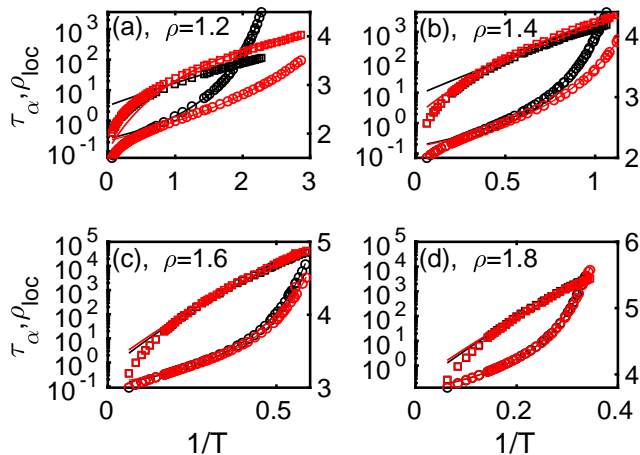


Figure 3.  $\tau_\alpha$  in semilog (left Y scale) versus  $1/T$ , by circles connected by VFT fit and  $\rho_{loc}$  in linear scale(right Y scale) versus  $1/T$  as (squares), lines are Eq. 2, for KA (black) and KAWCA (red) models.

the unavailability of kinetic energy that prevents particles from escaping from the potential energy minima and thus forms a cage. This cage exerts a fluctuating force on any reference particle whose mean at position  $r^*$  quantifies the barrier for a confined particle. The mean force exerted on a reference particle by density at  $r$  in the radial direction is  $F(r) = \frac{1}{N\rho} \sum_{\alpha\beta} |F_{\alpha\beta}(r)\hat{r}|$ , where  $F_{\alpha\beta}(r)\hat{r} = \mathbf{f}_{\alpha\beta}(r)n_{\alpha\beta}(r)$  and,  $\mathbf{f}_{\alpha\beta}(r) = -\frac{\partial V_{\alpha\beta}(r)}{\partial r}\hat{r}$ , where  $n_{\alpha\beta}$  is unnormalized pair density.  $F(r)$  at the highest peak in Fig. 1(d) at  $\rho=1.2$ , differ for KAWCA and KA: plot of the difference in forces  $\Delta F(r)$  in these models is in the inset of fig.1(d). The  $\Delta F(r)$  reduces at high densities  $\rho=1.8$ . Next these growths in  $g(r^*)$  and  $F(r^*)$  in KA and KAWCA models are compared with the density relaxation time. We get the estimate of the density relaxation time  $\tau_\alpha$  by integrating the incoherent intermediate scattering function  $F_s(k,t)$ [13],  $\tau_\alpha = \int_0^\infty F_s(k,t)dt$  at  $k=7.28$ , where  $k$  is the mean wavenumber at the first peak of  $S(k)$ ; see Fig. 3(a-d). The difference in mean force on particles in these models shows a difference in relaxation in earlier studies [11, 12]. The increase of  $\rho_{loc}$  results in a corresponding exponential increase of  $\tau_\alpha$  as the temperature in fig 3, which is due to an increase in the jamming of particles in the relaxation channel marked with black arrows in fig.1(b). Studies of the structure near jamming transition in repulsive 3D colloidal systems show that  $g(r)$  grows systematically near jamming [44]. The signatures of jamming appear in the force distribution of bio-polymers [45] predominantly due to attractive interaction.

The free-volume change in the spherical shell  $N_m/(\rho_0 - \rho_{loc})$ , where  $N_m$  is the mean shell occupation in the supercooled state and  $\rho_0$  is the maximum value  $\rho_{loc}$  attains by decrease of  $T$  for a particular  $V$ , beyond which relaxation time diverges. Note that in the supercooled

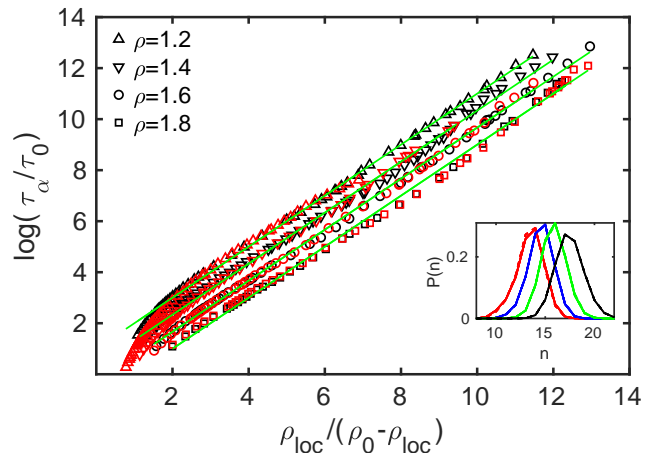


Figure 4. The collapsed plot of the logarithm of scaled relaxation time versus relative variation of the local density  $\rho_{loc}$  for KA (black) and KAWCA (red) models (shifted for clarity). Inset shows nearest neighbor distribution  $P(n)$  with in radius  $1.4\sigma_{AA}$  for all densities in multiple supercooled states which overlap for a constant  $\rho$ . In the inset, the density increase from left to right for KA(—) KAWCA(---).

state, nearest neighbor distribution  $P(n)$  overlaps for many temperatures for both models at a particular  $\rho$ ; see the inset of Fig. 4; implying  $N_m$  is constant in the supercooled state. There is negligible variation in the number of particles in a spherical shell of infinitesimal thickness with  $r^* \simeq \text{constant}$  (fig. 4(inset)). This free volume in a shell with radius  $r^*$  gives an estimate of the overall free volume, which assists the density relaxation. Then the relaxation time from free-volume theory is modified with  $v_0 = N_m/\rho_0$  as a function of  $\rho_{loc}$  reads

$$\tau_\alpha = \tau_\rho e^{\left(\frac{Bv_0}{v-v_0}\right)} \simeq \tau_\rho e^{\left(\frac{B\rho_{loc}}{\rho_0 - \rho_{loc}}\right)}. \quad (1)$$

A fit of this relation in KA and KAWCA models for Fig. 4 show  $B \sim 1$  [46]. The deviation of the simulation data from Eq.1 is due to the non-monotonous increase of  $r^*$  in Fig. 2 due to the formation of local structures that affect the shape of the cages. Moreover, the assumption of a perfectly spherical barrier of the cage marked by circles in 1(b) is the nearest approximation of the collective potential barrier of a molecular cage. Note that the relaxation time fluctuates around a straight line in Fig. 4, showing that this relation holds reasonably well. Also, a system of linear supercooled flexible polymers obeys an equation which is similar to Eq. 1 [47]. The eq. 1 is similar to the Vogel-Fulcher-Tammann (VFT) relation  $\tau_\alpha = \tau_T \exp(A/(T - T_0))$ , where  $A$  and  $T_0$  are constants. Earlier experimental studies show that the free volume is a function of temperature  $v_f^* = C + k(T - T_g)$  with constants  $k$  and  $C$ , where  $C$  is the excess free-volume at  $T_g$  [46, 48]. With the new definition of free-volume of a pair of neighbors,  $v_f \propto (T - T_0)$  as  $\rho_{loc}$  increase till  $T_0$ . Many studies use an alternative representation of

the free volume as a function of the Debye-Waller factor  $\langle u^2 \rangle$  [27, 49–51], which shows an exponential increase of density relaxation time with  $\langle u^2 \rangle$ , which is comparable to Eq.1 [47]; thus suggest a relation between  $\rho_{loc}$  and  $\langle u^2 \rangle$ . A study of string-like motion in the polymer models show  $\langle u^2 \rangle$  vanish at  $T_0$  [52]. Thus equating the Eq. 1 and VFT expression yields a relation between  $\rho_{loc}$  and temperature difference reads

$$\rho_{loc} = \rho_0 \left[ \frac{k(T - T_0) - A}{(k - 1)(T - T_0) - A} \right], \quad (2)$$

where constant  $k = \ln(\tau_\rho/\tau_T)$ . In the supercooled liquids Eq. 2 is valid; that is evident from the plot of Eq. 2 in Fig. 3, which shows that the VFT relation is related to jamming of particles due to density enhancement, below this temperature dynamics diverge significantly, arresting the density relaxation.

In summary, these studies show a direct correlation between the local density and the radial forces, and the density relaxation dynamics. These results, when combined with string-like excitation [30–33] and Flory’s mean-field theory of polymer relaxation based on the free-volume [39, 40, 43] connects surface density at the peak of the  $g(r^*)$  in the first-coordination shell and the density relaxation time  $\tau_\alpha$  in Eq.1. The VFT-like structure of the Eq. 1 is in agreement with a similar relation for an order parameter derived among the angle between particles in the first coordination shell [17], which is valid in 2D as well. Therefore, the results of this study provide a model connecting local density and density relaxation in nonassociated liquids [53].

We thank the HPC facility at IIT Mandi for computational facilities. The School of Physical Sciences is bifurcation of the former School of Basic Sciences at IIT Mandi, where DCT, JS, and AV are affiliated during this work.

---

\* [prasanth@iitmandi.ac.in](mailto:prasanth@iitmandi.ac.in)

- [1] B. Li, K. Lou, W. Kob, and S. Granick, *Nature* **587**, 225 (2020).
- [2] R. Pastore, G. Pesce, A. Sasso, and M. P. Ciamarra, *J. Phys. Chem. Lett.* **8**, 1562 (2017).
- [3] J. D. Weeks, D. Chandler, and H. C. Andersen, *J. Chem. Phys.* **54**, 5237 (1971).
- [4] D. Chandler, *Acc. Chem. Res.* **7**, 246 (1974).
- [5] W. Kob and H. C. Andersen, *Phys. Rev. Lett.* **73**, 1376 (1994).
- [6] T. A. Weber and F. H. Stillinger, *Phys. Rev. B* **31**, 1954 (1985).
- [7] L. Berthier and G. Tarjus, *Phys. Rev. Lett.* **103**, 170601 (2009).
- [8] L. Berthier and G. Tarjus, *J. Chem. Phys.* **134**, 214503 (2011).
- [9] S. Toxvaerd and J. C. Dyre, *J. Chem. Phys.* **135**, 134501 (2011).
- [10] U. R. Pedersen, T. B. Schroder, and J. C. Dyre, *Phys. Rev. Lett.* **105**, 157801 (2010).
- [11] L. Bohling, A. A. Veldhorst, T. S. Ingebrigtsen, N. P. Bailey, J. S. Hansen, S. Toxvaerd, T. B. Schroder, and J. C. Dyre, *J. Phys.: Condens. Matter* **25**, 032101 (2013).
- [12] J. Chattoraj and M. P. Ciamarra, *Phys. Rev. Lett.* **124**, 028001 (2020).
- [13] J. P. Hansen and I. R. McDonald, *Theory of simple liquids* (Academic Press, London, 1986).
- [14] A. Banerjee, S. Sengupta, S. Sastry, and S. M. Bhattacharyya, *Phys. Rev. Lett.* **113**, 225701 (2014).
- [15] A. Singh and Y. Singh, *Phys. Rev. E* **103**, 052105 (2021).
- [16] F. P. Landes, G. Biroli, O. Dauchot, A. J. Liu, and D. R. Reichman, *Phys. Rev. E* **101**, 010602 (2020).
- [17] H. Tong and H. Tanaka, *Phys. Rev. Lett.* **124**, 225501 (2020).
- [18] U. Bengtzelius, W. Gotze, and A. Sjolander, *J. Phys. C: Solid State Phys.* **17**, 5915 (1984).
- [19] L. Berthier and G. Biroli, *Rev. Mod. Phys.* **83**, 587 (2011).
- [20] S. Karmakar, C. Dasgupta, and S. Sastry, *Phys. Rev. Lett.* **116**, 085701 (2016).
- [21] R. L. Jack, A. J. Dunleavy, and C. P. Royall, *Phys. Rev. Lett.* **113**, 095703 (2014).
- [22] J. Singh and P. P. Jose, *J. Phys.: Condens. Matter* **33**, 055401 (2021).
- [23] M. R. Hasyim and K. K. Mandadapu, *J. Chem. Phys.* **155**, 044504 (2021).
- [24] D. Chandler and J. P. Garrahan, *Ann. Rev. Phys. Chem.* **61**, 191 (2010).
- [25] G. S. Grest and M. H. Cohen, *Adv. Chem. Phys.* **48**, 455 (1981).
- [26] D. Turnbull and M. H. Cohen, *J. Chem. Phys.* **29**, 1049 (1958).
- [27] F. W. Starr, S. Sastry, J. F. Douglas, and S. C. Glotzer, *Phys. Rev. Lett.* **89**, 125501 (2002).
- [28] R. P. White and J. E. G. Lipson, *Macromolecules* **49**, 3987 (2016).
- [29] M. P. Allen and D. J. Tildesley, *Computer simulation of liquids* (Oxford University Press, New York, 1991).
- [30] W. Kob, C. Donati, S. J. Plimpton, P. H. Poole, and S. C. Glotzer, *Phys. Rev. Lett.* **79**, 2827 (1997).
- [31] C. Donati, S. C. Glotzer, P. H. Poole, W. Kob, and S. J. Plimpton, *Phys. Rev. E* **60**, 3107 (1999).
- [32] M. Aichele, Y. Gebremichael, F. W. Starr, J. Baschnagel, and S. C. Glotzer, *J. Chem. Phys.* **119**, 5290 (2003).
- [33] C.-T. Yip, M. Isobe, C.-H. Chan, S. Ren, K.-P. Wong, Q. Huo, C.-S. Lee, Y.-H. Tsang, Y. Han, and C.-H. Lam, *Phys. Rev. Lett.* **125**, 258001 (2020).
- [34] J. D. Stevenson and P. G. Wolynes, *Nat. Phys.* **6**, 62 (2010).
- [35] J. F. Douglas and W.-S. Xu, *Macromolecules* **54**, 3247 (2021).
- [36] J. D. Stevenson, J. Schmalian, and P. G. Wolynes, *Nat. Phys.* **2**, 268 (2006).
- [37] Z. Zhang, P. J. Yunker, P. Habdas, and A. G. Yodh, *Phys. Rev. Lett.* **107**, 208303 (2011).
- [38] K. H. Nagamanasa, S. Gokhale, A. K. Sood, and R. Ganapathy, *Nat. Phys.* **11**, 403 (2015).
- [39] J. S. Langer and A. Lemaitre, *Phys. Rev. Lett.* **94**, 175701 (2005).
- [40] J. S. Langer, *Phys. Rev. E* **73**, 041504 (2006).
- [41] T. Salez, J. Salez, K. Dalnoki-Veress, E. Raphael, and J. A. Forrest, *Proc. Natl. Acad. Sci.* **112**, 8227 (2015).

- [42] S. Swayamjyoti, J. F. Loffler, and P. M. Derlet, *Phys. Rev. B* **89**, 224201 (2014).
- [43] P. J. Flory, *Principles of Polymer Chemistry* (Cornell University Press, Ithaca, NY, 1953).
- [44] Z. Zhang, N. Xu, D. T. N. Chen, P. Yunker, A. M. Alsayed, K. B. Aptowicz, P. Habdas, A. J. Liu, S. R. Nagel, and A. G. Yodh, *Nature* **459**, 230 (2009).
- [45] P. P. Jose and I. Andricioaei, *Nat. Comm.* **3**, 1161 (2012).
- [46] A. K. Doolittle, *J. App. Phys.* **22**, 1471 (1951).
- [47] J. Singh, D. C. Thakur, and P. P. Jose, *AIP Conference Proceedings* **2265**, 030220 (2020).
- [48] M. L. Williams, R. F. Landel, and J. D. Ferry, *J. Am. Chem. Soc.* **77**, 3701 (1955).
- [49] R. W. Hall and P. G. Wolynes, *J. Chem. Phys.* **86**, 2943 (1987).
- [50] D. S. Simmons, M. T. Cicerone, Q. Zhong, M. Tyagi, and J. F. Douglas, *Soft Matter* **8**, 11455 (2012).
- [51] L. Larini, A. Ottochian, D. Michele, and D. Leporini, *Nat. Phys.* **4**, 42 (2008).
- [52] B. A. P. Betancourt, F. W. Starr, and J. F. Douglas, *J. Chem. Phys.* **148**, 104508 (2018).
- [53] D. Chandler, *Introduction to modern statistical mechanics* (Oxford University press, Oxford, U. K., 1987).